

# Journal of Biomedical Optics

BiomedicalOptics.SPIEDigitalLibrary.org

## **Characterization of natural and irradiated nails by means of the depolarization metrics**

Sergey Savenkov  
Alexander Priezzhev  
Yevgen Oberemok  
Sergey Sholom  
Ivan Kolomiets  
Kateryna Chunikhina

# Characterization of natural and irradiated nails by means of the depolarization metrics

Sergey Savenkov,<sup>a,\*</sup> Alexander Priezzhev,<sup>b</sup> Yevgen Oberemok,<sup>a</sup> Sergey Sholom,<sup>c</sup> Ivan Kolomiets,<sup>a</sup> and Kateryna Chunikhina<sup>a</sup>

<sup>a</sup>Taras Shevchenko National University of Kyiv, Faculty of Radio Physics, Electronics and Computer Systems, Vladimirskaya Street 64, Kiev 01033, Ukraine

<sup>b</sup>Lomonosov Moscow State University, Department of Physics and International Laser Center, Vorobiovy Gory, Moscow 119992, Russia

<sup>c</sup>Oklahoma State University, Department of Physics, 145 Physical Sciences Building, Stillwater, Oklahoma 74078, United States

**Abstract.** Mueller polarimetry is applied to study the samples of nails: natural (or reference) and irradiated to 2 Gy ionizing radiation dose. We measure the whole Mueller matrices of the samples as a function of the scattering angle at a wavelength of 632.8 nm. We apply depolarization analysis to measured Mueller matrices by calculating the depolarization metrics [depolarization index, Q(M)-metric, first and second Lorenz indices, Cloude and Lorenz entropy] to quantify separability of the different samples of nails under study based on differences in their Mueller matrix. The results show that nail samples strongly depolarize the output light in backscattering, and irradiation in all cases results in increasing of depolarization. Most sensitive among depolarization metrics are the Lorenz entropy and Q(M)-metric. © 2016 Society of Photo-Optical Instrumentation Engineers (SPIE) [DOI: 10.1117/1.JBO.21.7.071108]

Keywords: light scattering; polarimeter; Mueller matrix; depolarization metrics; radiation dose.

Paper 150655SSR received Oct. 1, 2015; accepted for publication Feb. 4, 2016; published online Feb. 26, 2016.

## 1 Introduction

Development in nuclear technologies and industry resulted in increasing number of radiation accidents, which usually are accompanied by exposure of significant number of general population to unpredictable ionizing radiation doses. Some examples of such accidents are disasters at the Chernobyl nuclear power plant in Ukraine (April 1986) and at the Fukushima Nuclear Power Plant in Japan (March 2011). In both accidents, hundreds of thousands of people were exposed to unknown doses.

In order to provide the adequate medical assistance to potential sufferers from a radiation accident, it is necessary to estimate their radiation doses using some dosimetric technique with some appropriate materials. This is not a trivial task, and until now there is no established dosimetric technique that could be used for emergency dose reconstruction. Two main physical methods are usually exploited, namely electron paramagnetic resonance (EPR) and optically-stimulated luminescence (OSL) techniques. They might be applied to some human tissues like teeth and nails<sup>1-5</sup> as well as to some materials/items which could be carried by an individual during emergency exposure. Materials potentially available for emergency dose reconstruction include different paper and plastic cards, banknotes, fabrics, shoes, resistors, integrated circuits, and displays of mobile phones.<sup>6-14</sup> Despite significant progress achieved with some materials using EPR and OSL techniques, there are too many limitations with their possible practical use for fast estimation of emergency doses, and search of new techniques and materials that could be used for emergency dose reconstruction is still an actual task.

In the present paper, we tested the Mueller polarimetry for the possible application for emergency dose assessment using the human nails. To that end, the complete Mueller matrices for three sets of nail's samples, reference, and irradiated, are measured in visible ( $\lambda = 632.8$  nm). After that, the parameters characterizing depolarization properties of the samples (depolarization metrics) have been calculated. Thereby, this study presents results for the use of depolarization metrics extractable from the experimental Mueller matrices to distinguish between natural and irradiated human nails and determines which of them are most sensitive for that.

In Sec. 2, we present a description of the Mueller experimental approach. Section 3 summarizes preparation features and characteristics of samples studied. In Sec. 4, we briefly review the parameters characterizing depolarization properties of a sample. Results and discussion of our experiments are given in Sec. 5.

## 2 Mueller Matrix Measurements

In polarimetry the most complete characterization of studied object is attained by measurement of the Mueller matrix of studied object.<sup>15-18</sup> At that, a light beam is characterized by the Stokes vector  $\mathbf{I} = (I \ Q \ U \ V)^T$ .<sup>19</sup> Its parameters present the total intensity ( $I$ ), linearly ( $Q$  and  $U$ ) and circularly ( $V$ ) polarized components. Scattering is described by the following matrix equation<sup>20</sup>

$$\mathbf{I}^{\text{out}} = \mathbf{M}\mathbf{I}^{\text{inp}}, \quad (1)$$

where  $\mathbf{I}^{\text{inp}}$  and  $\mathbf{I}^{\text{out}}$  are the Stokes vectors of input and output (scattered) light;  $\mathbf{M}$  is the Mueller matrix of studied object

\*Address all correspondence to: Sergey Savenkov, E-mail: [sns@univ.kiev.ua](mailto:sns@univ.kiev.ua)

depending on wavelength, incident, and scattering directions and properties of the object. The analysis of the depolarization and anisotropy information contained in the Mueller matrix  $\mathbf{M}$  provides one with valuable information on structure and properties of examined objects.

The Mueller matrix polarimeter is composed of a polarization state generator (PSG) and polarization state analyzer (PSA).<sup>20,21</sup> The PSG generates the particular polarization states of light impinging on the studied sample. The PSA measures the full or certain of parameters of scattered light's Stokes vector. Both PSG and PSA consist of retarders and diattenuators that are capable of analyzing the polarization state of the scattered beam.

For any PSG and PSA, the total flux measured by the detector is

$$g = \mathbf{QML} = \sum_{i=1}^4 \sum_{j=1}^4 q_i m_{ij} l_j, \quad (2)$$

where  $\mathbf{L}$  is the Stokes vector produced by PSG;  $\mathbf{M}$  is the object Mueller matrix;  $\mathbf{Q}$  is the Stokes vector corresponding to the first row of the Mueller matrix representing the PSA.

To measure the full Mueller matrix,  $N = 16$  flux measurements, according to Eq. (2), are required. Representing the Mueller matrix  $\mathbf{M}$  as a  $16 \times 1$  vector of the form  $\vec{\mathbf{M}} = [m_{11} \ m_{12} \ m_{13} \ m_{14} \ \cdot \ \cdot \ \cdot \ m_{43} \ m_{44}]^T$  the polarimetric measurement equation can be expressed as follows

$$\mathbf{G} = \mathbf{WM} = \begin{pmatrix} q_1^1 l_1^1 & q_1^1 l_2^1 & q_1^1 l_3^1 & \cdot & q_4^1 l_4^1 \\ q_1^2 l_1^2 & q_1^2 l_2^2 & q_1^2 l_3^2 & \cdot & q_4^2 l_4^2 \\ q_1^3 l_1^3 & q_1^3 l_2^3 & q_1^3 l_3^3 & \cdot & q_4^3 l_4^3 \\ \cdot & \cdot & \cdot & \cdot & \cdot \\ q_1^N l_1^N & q_1^N l_2^N & q_1^N l_3^N & \cdot & q_4^N l_4^N \end{pmatrix} \begin{pmatrix} m_{11} \\ m_{12} \\ m_{13} \\ \cdot \\ m_{44} \end{pmatrix}, \quad (3)$$

where  $\mathbf{G}$  is the  $N \times 1$  vector, whose components are the fluxes measured by detector;  $\mathbf{W}$  is  $N \times 16$  general characteristic or data reduction matrix with elements  $w_{ij}^N = q_i^N l_j^N$ .

If PSG and PSA are configured so that  $\mathbf{W}$  is of rank sixteen, then all sixteen Mueller matrix elements can be determined in such a way

$$\vec{\mathbf{M}} = \mathbf{W}^{-1} \mathbf{G}. \quad (4)$$

Particular scheme of Mueller polarimeter used in this experiment is shown in Fig. 1.

Light beam from a linearly polarized continuous-wave He-Ne laser (1) passes through a polarization state generator PSG consisting of polarizer (2) and two LC wave plates (3) with phase shifts  $\delta_1, \delta_2$  and azimuths  $\alpha_1, \alpha_2$ . The light is subsequently scattered by a sample (4). Then scattered light passes through a polarization state analyzer (PSA) consisting of rotatable crystalline wave plate (5) with phase shift  $\delta_3$  and an analyzer (6) and is measured by a detector (7), so that PSA is a complete Stokes polarimeter.<sup>21,22</sup> Polarizer (2) and analyzer (6) are fixed and crossed relative to each other. The wave plates in PSG and PSA are assembled by holders controlled from the computer.

Thus, the polarimeter, Fig. 1 realizes the so called time-sequential measurement strategy.<sup>21,23</sup> This allows considering the parameters of vector  $\mathbf{G}$  in Eq. (3) as parameters of the

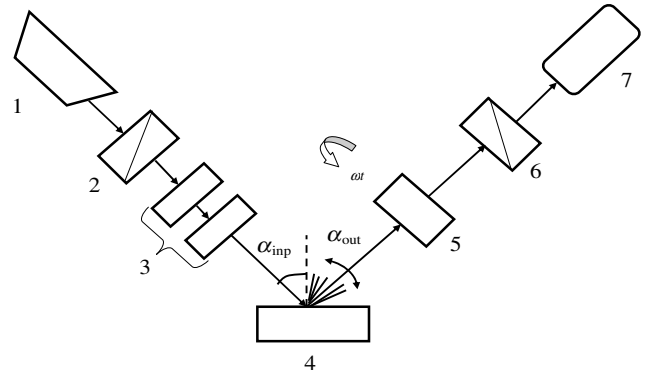


**Fig. 1** Schematic overview of the experimental geometry to measure the Mueller matrices.

Stokes vectors measured by PSA. In this case characteristic matrix  $\mathbf{W}$  in Eq. (3) takes a block-diagonal form

$$\mathbf{W}_{16 \times 16} = \begin{pmatrix} \mathbf{V} & 0 & 0 & 0 \\ 0 & \mathbf{V} & 0 & 0 \\ 0 & 0 & \mathbf{V} & 0 \\ 0 & 0 & 0 & \mathbf{V} \end{pmatrix}, \quad (5)$$

with  $4 \times 4$  block matrix of the form

$$\mathbf{V} = \begin{pmatrix} r_1^1 & r_2^1 & r_3^1 & r_4^1 \\ r_1^2 & r_2^2 & r_3^2 & r_4^2 \\ r_1^3 & r_2^3 & r_3^3 & r_4^3 \\ r_1^4 & r_2^4 & r_3^4 & r_4^4 \end{pmatrix}, \quad (6)$$

where  $r_i^k$  is the  $i$ 'th parameter of  $k$ 'th Stokes vector,  $k = \overline{1,4}$ , generated by PSG.

In this experiment, we use the following set of optimal polarizations minimizing the condition number of block matrix Eq. (6)<sup>23</sup>

$$\mathbf{V}_{4 \times 4} = \begin{pmatrix} 1 & 1 & 0 & 0 \\ 1 & -0.333 & -0.816 & 0.471 \\ 1 & -0.333 & 0 & -0.943 \\ 1 & -0.333 & 0.816 & 0.471 \end{pmatrix}. \quad (7)$$

### 3 Samples

Nails for this study were obtained from three volunteers, denoted below as AL (a on the plots), F23 (b on the plots), JOE (c on the plots). Nails were collected during routine hygienic procedures and were stored at ambient conditions between clipping and submitting to the research laboratory.

Large aliquots of the size approximately  $3 \times 3$  mm<sup>2</sup> were cut from the originally collected nail clips for consecutive exposure and measurement with a polarimetric technique. Samples were exposed on a 250 mCi <sup>90</sup>Sr/<sup>90</sup>Y beta source located at the Radiation Dosimetry Laboratory of Oklahoma State University. The source was calibrated against a National Institute of Standards and Technology secondary standard <sup>60</sup>Co source in terms of absorbed doses to water using Luxel Al<sub>2</sub>O<sub>3</sub>:C OSL dosimeters. Samples were exposed at the dose rate of 0.26 Gy/s.

Immediately after irradiation, samples were sent to the research laboratory in Kiev using an express mail service; samples were tested at 5 days after exposure.

#### 4 The Depolarization Metrics

In this Section, we review briefly the parameters used in this experiment for characterization of the depolarization of the samples under consideration—depolarization metrics. The depolarization metrics provide a summary of the depolarizing property of a sample via a single number that varies from zero, thereby corresponding to a totally depolarized output light, to a certain positive number corresponding to a totally polarized output light. All intermediate values are associated with partial polarization.

The most commonly used metric is the depolarization index  $DI(\mathbf{M})$  proposed more than 20 years ago by Gil and Bernabeu,<sup>24,25</sup>

$$DI(\mathbf{M}) = \sqrt{\frac{\sum_{i,j=1}^4 m_{ij}^2 - m_{11}^2}{(\sqrt{3}m_{11})}}. \quad (8)$$

The depolarization index is bounded according to  $0 \leq DI(\mathbf{M}) \leq 1$ . The extreme values of  $DI(\mathbf{M})$  correspond to the case of unpolarized and totally polarized output light, respectively.

The so-called  $Q(\mathbf{M})$  metrics is defined as follows<sup>26</sup>

$$Q(\mathbf{M}) = \frac{\sum_{i=2}^4 \sum_{j=1}^4 m_{ij}^2}{\sum_{j=1}^4 m_{1j}^2} = \frac{3[DI(\mathbf{M})]^2 - [D(\mathbf{M})]^2}{1 + [D(\mathbf{M})]^2}, \quad (9)$$

where  $D(\mathbf{M}) = (m_{12}^2 + m_{13}^2 + m_{14}^2)^{1/2}/m_{11}$  is the diattenuation parameter and  $0 \leq D(\mathbf{M}) \leq 1$ . The metric  $Q(\mathbf{M})$  is bounded according to  $0 \leq Q(\mathbf{M}) \leq 3$ . Specifically,  $Q(\mathbf{M}) = 0$  corresponds to a totally depolarizing medium;  $0 < Q(\mathbf{M}) < 1$  describes a partially depolarizing medium;  $1 \leq Q(\mathbf{M}) < 3$  represents a partially depolarizing medium if, in addition,  $0 < DI(\mathbf{M}) < 1$ ; otherwise, it represents a depolarizing diattenuating medium; finally,  $Q(\mathbf{M}) = 3$  for a nondepolarizing non-diattenuating medium.

Depolarization metrics named first and second Lorentz depolarization indices

$$L1 = \sqrt{\frac{\text{tr}(\mathbf{N}) - \rho_{\max}}{3\rho_{\max}}}, \quad (10)$$

$$L2 = \sqrt{\frac{4\text{tr}(\mathbf{N}^2) - \text{tr}^2(\mathbf{N})}{3\text{tr}^2(\mathbf{N})}}, \quad (11)$$

are proposed in Ref. 27. Here

$$\mathbf{N} = \mathbf{GM}^T \mathbf{GM}, \quad (12)$$

and

$$\mathbf{G} = \begin{pmatrix} 1 & 0 & 0 & 0 \\ 0 & -1 & 0 & 0 \\ 0 & 0 & -1 & 0 \\ 0 & 0 & 0 & -1 \end{pmatrix}, \quad (13)$$

is the Minkowski metric;  $\rho_{\max}$  is the maximum eigenvalue of  $\mathbf{N}$ . Metric  $L1$  is equal to 1 for a nondepolarizing  $\mathbf{M}$  and to less than 1, otherwise; it will be equal to zero for the ideal depolarizer  $\mathbf{M}_{ID} = \text{diag}(1 \ 0 \ 0 \ 0)$ . At the same time, the metric  $L2 = 0$  for a nondepolarizing  $\mathbf{M}$ ,  $L2 = 1$  for  $\mathbf{M}_{ID}$ , and take intermediate values, otherwise.

Another metric characterizing depolarization properties of a sample is deduced basing on the coherency matrix suggested by Cloude in Refs. 28 and 29 and extensively employed in optical polarimetry and remote sensing.<sup>30-37</sup> The Cloude coherency matrix  $\mathbf{J}$  is derived from the corresponding arbitrary Mueller matrix as follows:

$$\begin{aligned} j_{11} &= 1/4(m_{11} + m_{22} + m_{33} + m_{44}), \\ j_{22} &= 1/4(m_{11} + m_{22} - m_{33} - m_{44}), \\ j_{33} &= 1/4(m_{11} - m_{22} + m_{33} - m_{44}), \\ j_{44} &= 1/4(m_{11} - m_{22} - m_{33} + m_{44}), \\ j_{14} &= 1/4(m_{14} - im_{23} + im_{32} + m_{41}), \\ j_{23} &= 1/4(im_{14} + m_{23} + m_{32} - im_{41}), \\ j_{32} &= 1/4(-im_{14} + m_{23} + m_{32} + im_{41}), \\ j_{41} &= 1/4(m_{14} + im_{23} - im_{32} + m_{41}), \\ j_{12} &= 1/4(m_{12} + m_{21} - im_{34} + im_{43}), \\ j_{21} &= 1/4(m_{12} + m_{21} + im_{34} - im_{43}), \\ j_{34} &= 1/4(im_{12} - im_{21} + m_{34} + m_{43}), \\ j_{43} &= 1/4(-im_{12} + im_{21} + m_{34} + m_{43}), \\ j_{13} &= 1/4(m_{13} + m_{31} + im_{24} - im_{42}), \\ j_{31} &= 1/4(m_{13} + m_{31} - im_{24} + im_{42}), \\ j_{24} &= 1/4(-im_{13} + im_{31} + m_{24} + m_{42}), \\ j_{42} &= 1/4(im_{13} - im_{31} + m_{24} + m_{42}). \end{aligned} \quad (14)$$

It can be seen that coherency matrix  $\mathbf{J}$  is positive semidefinite Hermitian and, hence, has always four real eigenvalues. This yields a requirement for the Mueller matrix to be physically realizable: the coherency matrix  $\mathbf{J}$  should have all non-negative eigenvalues.<sup>28</sup> For the average characterization of depolarization for given Mueller matrix the following metric, called Cloude entropy, can be used

$$H = \sum_{i=1}^4 -P_i \log_4 P_i, \quad (15)$$

where

$$P_i = \frac{\lambda_i}{\sum_j \lambda_j}, \quad (16)$$

and  $\lambda_i$  are the eigenvalues of coherency matrix  $\mathbf{J}$  Eq. (14).

For pure scattering without depolarization,  $H = 0$  and  $\lambda_1 \neq 0$ ,  $\lambda_{i \neq 1} = 0$ . For totally depolarizing scatterers,  $H = 1$ . When  $H < 0.5$  and  $H > 0.5$ , one have weakly and strongly depolarizing cases, respectively.

The parameter analogues to the Cloude entropy  $H$ —Lorentz entropy  $HL$ —can also be derived using the eigenvalues  $\rho_i$  of matrix  $\mathbf{N}$  Eq. (12)<sup>27</sup>

$$HL = \sum_{i=1}^4 -\rho_i \log_4 \rho_i. \quad (17)$$

As it results from Eq. (17) the quantity  $HL = 1$  for a non-depolarizing  $\mathbf{M}$  and  $HL < 1$ , otherwise.

Given eigenvalues  $\lambda_i$  of coherency matrix  $\mathbf{J}$ , we have for initial Mueller matrix

$$\mathbf{M} = \sum_{k=1}^4 \lambda_k \mathbf{M}^k. \quad (18)$$

Here  $\mathbf{M}^k$  are the pure Mueller matrices derivable from corresponding Jones matrices.<sup>17,20,38</sup>

The Jones matrix,  $\mathbf{T}$ , in turn, is obtained in the following manner

$$\begin{aligned} t_{11}^{(k)} &= \Psi_1^{(k)} + \Psi_2^{(k)}, & t_{12}^{(k)} &= \Psi_3^{(k)} - i\Psi_4^{(k)} \\ t_{21}^{(k)} &= \Psi_3^{(k)} + i\Psi_4^{(k)}, & t_{22}^{(k)} &= \Psi_1^{(k)} - \Psi_2^{(k)}, \end{aligned} \quad (19)$$

where  $\Psi^{(k)} = (\Psi_1 \ \Psi_2 \ \Psi_3 \ \Psi_4)^T$  is  $k$ 'th eigenvector of coherence matrix  $\mathbf{J}$ .

Thus, the substance of the Cloude coherency matrix concept, which, in essence, is an additive matrix model of arbitrary depolarizing Mueller matrix, is the representation of the initial depolarizing Mueller matrix as a weighted sum of four pure Mueller matrices, see Eq. (18).

Evidently, the depolarization metrics presented above do not exhaust all known metrics characterizing the depolarization properties of a sample.<sup>39</sup> We confine ourselves in this Section only to the depolarization metrics, which are directly related to the Mueller matrix elements and need no scanning of whole Poincare sphere of input polarizations. These depolarization metrics are used in what follows.

## 5 Results and Discussion

Using the experimental setup described in Sec. 2 we measure the complete Mueller matrices of three sets of human nails and calculate the values of all depolarization metrics discussed in Sec. 4.

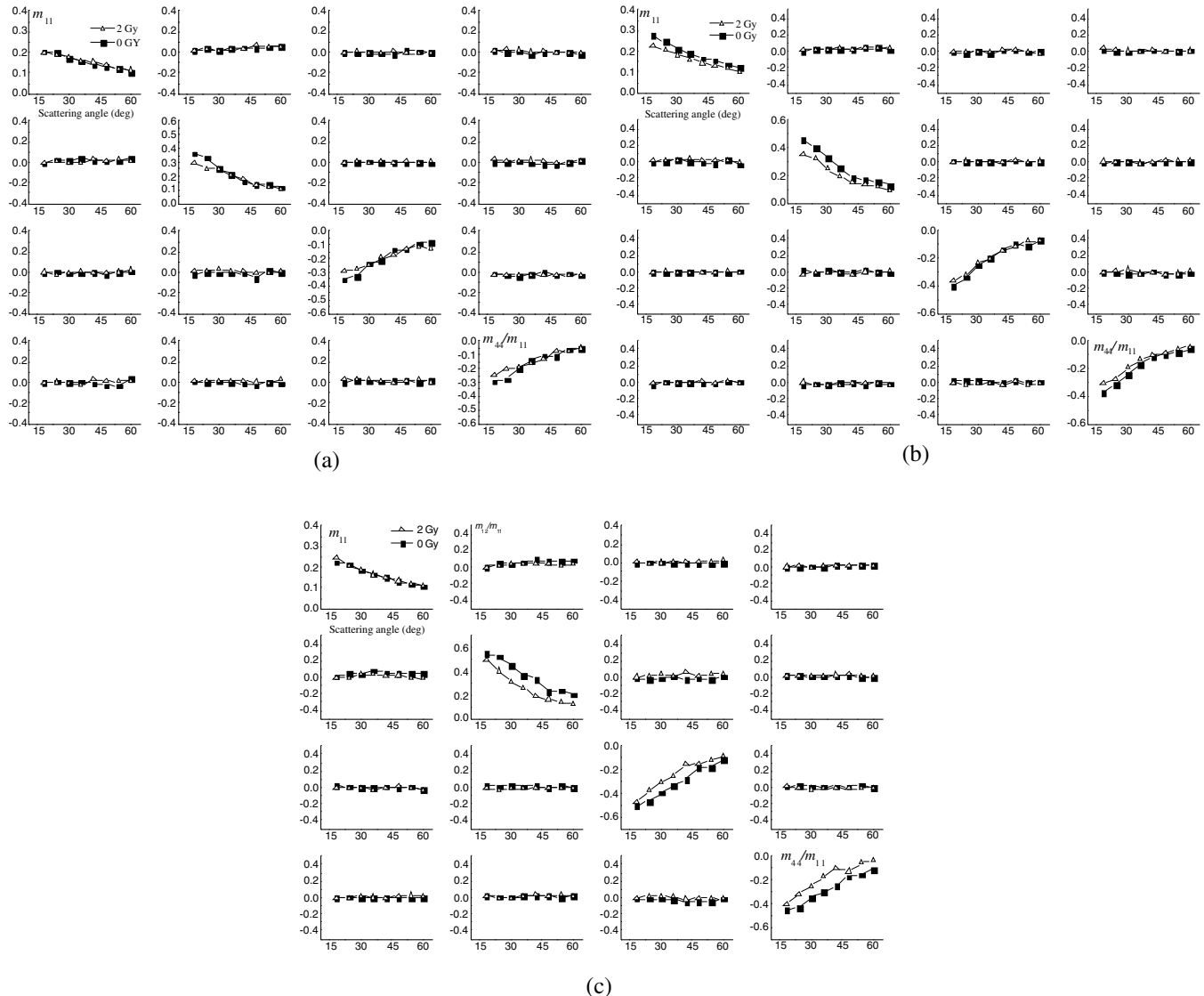


Fig. 2 Mueller matrix elements for nail samples: (a) AL, (b) F23, and (c) JOE.

In the experiment, the laser beam (15 mW) was widened up to 2 mm in diameter and directed to the external nail's surface in order to simulate the possible "in vivo" application of the polarimetric technique. Polarimetric properties of a reflected (from a nail surface) light were examined, which also attempted to follow the possible *in vivo* dose reconstruction protocol.

Prior to sample Mueller matrix measurement, the polarimeter was calibrated to obtain experimentally the optimum characteristic matrix Eq. (7). Figure 2 shows the measured Mueller matrix elements as functions of scattering angle for all samples.

Each point presented in the figures below is a result of averaging over 500 realizations of the single measurements. Except for  $m_{11}$  all matrix elements are normalized to  $m_{11}$ , so that we consider  $m_{ij}/m_{11}$ , with  $i, j = 1, 4$  aside from  $i = j = 1$ .

There are no error bars shown in Fig. 2 and in subsequent figures because experimentally estimated values of the standard deviations are comparable with the symbols plotted and below 2%. To avoid potential calculation problems we investigated the reliability of the measured scattering matrices by checking that all of them satisfy the Cloude test<sup>28</sup> within the experimental errors at each scattering angle. As it can be seen in the eight matrix elements  $m_{13}$ ,  $m_{14}$ ,  $m_{23}$ ,  $m_{24}$ ,  $m_{31}$ ,  $m_{32}$ ,  $m_{41}$  and  $m_{42}$  are zero within the experimental errors over the entire scattering angle range and, thus, the Mueller matrix has a block-diagonal structure. This structure of the Mueller matrix is characteristic for many scattering problems.<sup>40,41</sup>

From Fig. 2, we can also deduce that most sensitive matrix elements for given samples characterization are diagonal elements, i.e.,  $m_{11}$ ,  $m_{22}$ ,  $m_{33}$ , and  $m_{44}$ . However, the dosage sensitivity of matrix elements is different for different sets of nails. The same is for ranges of scattering angles characterized by maximum sensitivity. For set JOE, this is almost entire range of scattering angles, while for sets AL and F23 they are approximately 18 deg–27 deg and 18 deg–35 deg, respectively. The phase function  $m_{11}$  is almost unchanged in the whole range of scattering angles for sets AL and JOE and manifests sensitivity for F23 in 18 deg–35 deg range of scattering angles.

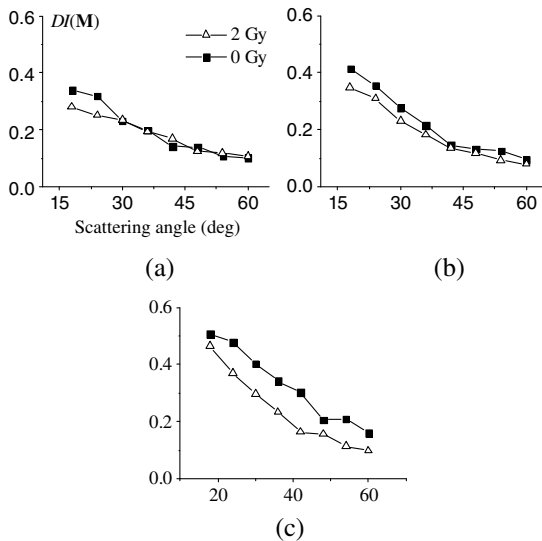


**Fig. 3** Dependence of depolarization index  $DI(\mathbf{M})$  on scattering angle: (a) AL, (b) F23, and (c) JOE.

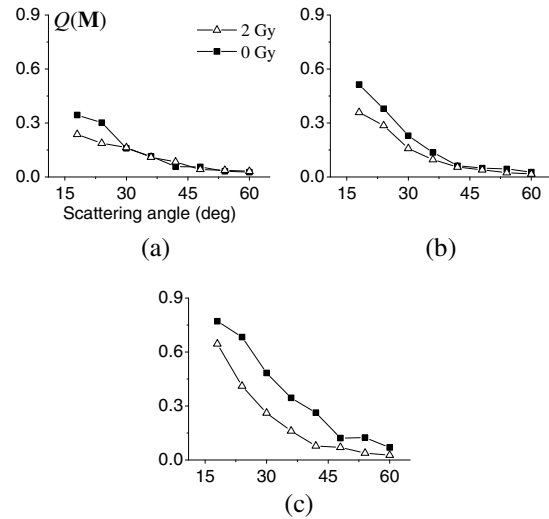


**Fig. 4** Dependence of  $Q(\mathbf{M})$ -metric on scattering angle: (a) AL, (b) F23, and (c) JOE.

Further, basing on the results of Mueller matrix measurements we examine the sensitivity of the depolarization metrics considered in Sec. 4.

Figures 3 and 4 show the behavior of depolarization index  $DI(\mathbf{M})$  and  $Q(\mathbf{M})$ -metric with altering the scattering angle. The similar dependences for first  $L1$  and second  $L2$  Lorentz depolarization indices are presented in Fig. 5 and, at last, the same for entropies  $H$  and  $HL$  is in Fig. 6.

As it can be seen all depolarization metrics show that nail samples depolarize strongly the output light in backscattering geometry (Fig. 1) and irradiation in all cases results in increasing of depolarization. This is presumably explained by strong

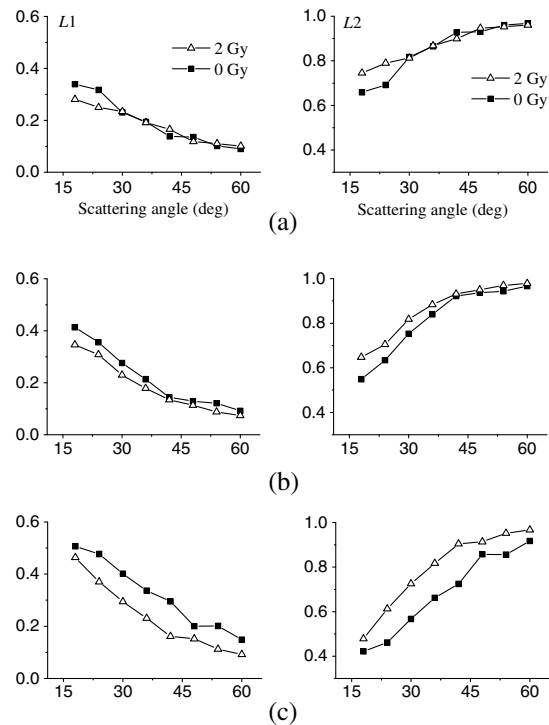


**Fig. 5** Dependence of first  $L1$  and second  $L2$  Lorentz depolarization indices on scattering angle: (a) AL, (b) F23, and (c) JOE.

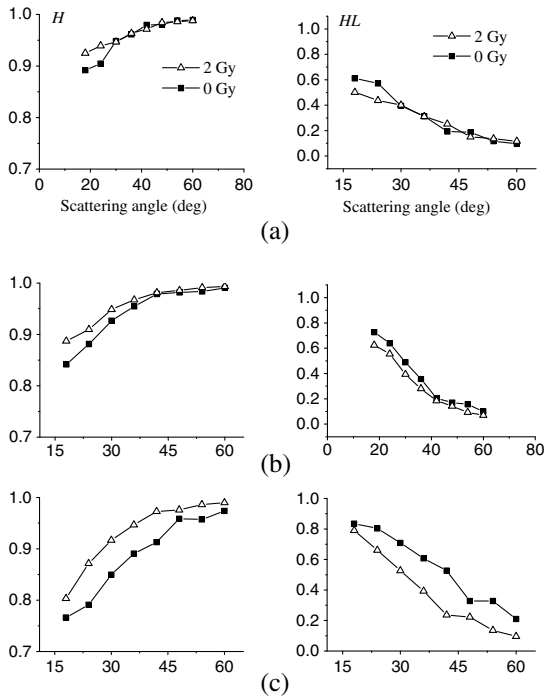


**Fig. 6** Dependence of entropies  $H$  and  $HL$  on scattering angle: (a) AL, (b) F23, and (c) JOE.

domination of volume scattering for scattering angles especially in the range  $18^\circ - 30^\circ$ . At the same time there exists an exception that is Lorenz entropy  $HL$ .  $HL$  shows that for small scattering angles  $18^\circ - 25^\circ$  samples of sets F23 and JOE depolarize weakly output light. However, the last one is not quite confirmed by the dependence of polarization degree on input polarization; see Fig. 7.

Depolarization metrics demonstrate a different ability to sample characterization with respect to the level of exposure dose. Evidently, most promising identifiers between reference and irradiated samples of nails are  $Q(\mathbf{M})$ -metric (Fig. 4) and entropy  $HL$  (Fig. 6).

Thus, the patterns of measured matrix elements and the results of subsequent interpretation of the experimental Mueller matrices show that Mueller polarimetry in visible enables to identify the reference and irradiated (in this experiment, this makes up 2 Gy) samples of nails. At that, it is important to note (see Fig. 7), that for better reliability of sample state distinction, one needs to examine all existing depolarization metrics jointly.

The reason why irradiated and nonirradiated samples of nails demonstrate different depolarizing ability cannot be determined within a framework of the current study. However, the following speculation may be proposed now. It is known from many publications (e.g., Refs. 2 and 42) that many different paramagnetic radicals are generated in nail tissue as a result of exposure to ionizing radiation. If these radicals have depolarizing properties different from those of original (precursor) molecules, this might be a reason of observed effects. Anyway, more experiments are required to understand this phenomenon.

All results accumulated up to date were obtained with only three samples (from three individuals). The further study will include the examination how variability in nails age, gender, and so on may influence the observed effects.

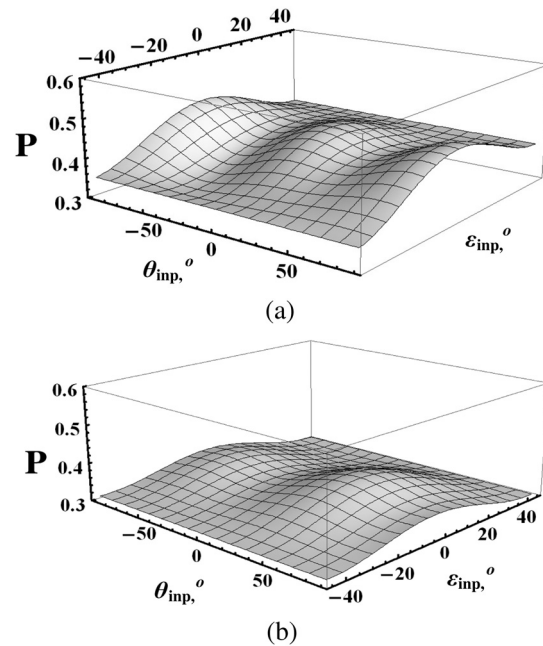


**Fig. 7** Dependence of polarization degree,  $P$ , for scattering angle  $18^\circ$  for set of nails F23 on azimuth  $\theta_{inp}$  and ellipticity  $\epsilon_{inp}$  of input light: (a) 0 Gy and (b) 2 Gy.

## References

1. B. B. Williams et al., "In vivo EPR tooth dosimetry for triage after a radiation event involving large populations," *Radiat. Environ. Biophys.* **53**(2), 335–346 (2014).
2. F. Trompier et al., "State of the art in nail dosimetry: free radicals identification and reaction mechanisms," *Radiat. Environ. Biophys.* **53**(2), 291–303 (2014).
3. S. Sholom et al., "Emergency dose estimation using optically stimulated luminescence from human tooth enamel," *Radiat. Meas.* **46**, 778–782 (2011).
4. S. Sholom et al., "Emergency optically stimulated luminescence dosimetry using different materials," *Radiat. Meas.* **46**, 1866–1869 (2011).
5. S. Sholom and M. Desrosiers, "EPR and OSL emergency dosimetry with teeth: a direct comparison of two techniques," *Radiat. Meas.* **71**, 494–497 (2014).
6. E. L. Inrig, D. I. Godfrey-Smith, and S. Khanna, "Optically stimulated luminescence of electronic components for forensic, retrospective and accident dosimetry," *Radiat. Meas.* **43**, 726–730 (2008).
7. C. Bassinet, F. Trompier, and I. Clairand, "Radiation accident dosimetry on electronic components by OSL," *Health Phys.* **98**(2), 440–445 (2010).
8. C. Bassinet et al., "Retrospective radiation dosimetry using OSL from electronic components: results of an inter-laboratory comparison," *Radiat. Meas.* **71**, 475–479 (2014).
9. A. Pascu et al., "The potential of luminescence signals from electronic components for accident dosimetry," *Radiat. Meas.* **56**, 384–388 (2013).
10. M. Discher and C. Woda, "Thermoluminescence of glass display from mobile phones for retrospective and accident dosimetry," *Radiat. Meas.* **53–54**, 12–21 (2013).
11. M. Discher, C. Woda, and I. Fiedler, "Improvement of dose determination using glass display of mobile phones for accident dosimetry," *Radiat. Meas.* **56**, 240–243 (2013).
12. P. Fattibene et al., "EPR dosimetry intercomparison using smart phone touch screen glass," *Radiat. Environ. Biophys.* **53**(2), 311–320 (2014).
13. S. Sholom and S. W. S. McKeever, "Emergency OSL dosimetry with commonplace materials," *Radiat. Meas.* **61**, 33–51 (2014).
14. S. Sholom and S. W. S. McKeever, "Emergency OSL/TL dosimetry with integrated circuits from mobile phones," *Proc. SPIE* **9213**, 921319 (2014).
15. A. A. Kokhanovsky, *Light Scattering Media Optics: Problems and Solutions*, Praxis Publishing, Chichester (2001).

16. A. Kokhanovsky, *Polarization Optics of Random Media*, Praxis Publishing, Chichester (2003).
17. M. I. Mishchenko, J. W. Hovenier, and L. D. Travis, *Light Scattering by Nonspherical Particles*, Academic Press, San Diego (2000).
18. V. V. Tuchin, L. V. Wang, and D. A. Zimnyakov, *Optical Polarization in Biomedical Applications*, Springer, Berlin (2006).
19. H. C. Van de Hulst, *Light Scattering by Small Particles*, Wiley, New York (1957).
20. C. Brosseau, *Fundamentals of Polarized Light: A Statistical Optics Approach*, Wiley, New York (1998).
21. R. A. Chipman, "Polarimetry," in *Handbook of Optics*, M. Bass, Ed., pp. 1–37, McGraw-Hill, New York (1995).
22. S. N. Savenkov et al., "Incomplete active polarimetry: measurement of the block-diagonal scattering matrix," *J. Quant. Spectrosc. Radiat. Transfer* **112**, 1796–1802 (2011).
23. S. N. Savenkov, "Optimization and structuring of the instrument matrix for polarimetric measurements," *Opt. Eng.* **41**, 965–972 (2002).
24. J. J. Gil and E. Bernabeu, "A depolarization criterion in Mueller matrices," *Opt. Acta* **32**, 259–261 (1985).
25. J. J. Gil and E. Bernabeu, "Depolarization and polarization indexes of an optical system," *Opt. Acta* **33**, 185–189 (1986).
26. R. Espinosa-Luna and E. Bernabeu, "On the Q(M) depolarization metric," *Opt. Commun.* **277**, 256–258 (2007).
27. R. Ossikovski, "Alternative depolarization criteria for Mueller matrices. Alternative depolarization criteria for Mueller matrices," *J. Opt. Soc. Am. A* **27**, 808–814 (2010).
28. S. R. Cloude and E. Pottier, "Concept of polarization entropy in optical scattering," *Opt. Eng.* **34**, 1599–1610 (1995).
29. S. R. Cloude, "Group theory and polarization algebra," *Optik(Stuttgart)* **75**(1), 26–36 (1986).
30. S. N. Savenkov, R. S. Muttiah, and Y. A. Oberemok, "Transmitted and reflected scattering matrices from an English oak leaf," *Appl. Opt.* **42**, 4955–4962 (2003).
31. S. N. Savenkov et al., "Mueller polarimetry of virus-infected and healthy wheat under field and microgravity conditions," *J. Quant. Spectrosc. Radiat. Transfer* **88**, 327–343 (2004).
32. H. Volten et al., "Scattering matrices of mineral aerosol particles at 441.6 nm and 632.8 nm," *J. Geophys. Res.* **106**, 375 (2001).
33. O. Munoz et al., "Experimental determination of scattering matrices of fly ash and clay particles at 442 and 633 nm," *J. Geophys. Res.* **106**, 22833 (2001).
34. O. Munoz et al., "Experimental determination of the phase function and degree of linear polarization of El Chichon and Pinatubo volcanic ashes," *J. Geophys. Res.* **107**, 715–718 (2002).
35. O. Munoz et al., "Scattering matrices of volcanic ash particles of Mount St. Helens, Redoubt, and Mount Spurr Volcanoes," *J. Geophys. Res.* **109**(D), 16201 (2004).
36. S. R. Cloude and E. Pottier, "A review of target decomposition theorems in radar polarimetry," *IEEE Trans. Geosci. Remote Sens.* **34**, 498–518 (1996).
37. S. R. Cloude and E. Pottier, "An entropy based classification scheme for land applications of polarimetric SAR," *IEEE Trans. Geosci. Remote Sens.* **35**, 68–78 (1997).
38. J. W. Hovenier, "Structure of a general pure Mueller matrix," *Appl. Opt.* **33**, 8318–8324 (1994).
39. S. N. Savenkov, "Jones and Mueller matrices: structure, symmetry relations and information content," in *Light Scattering Reviews 4 (Single Light Scattering and Radiative Transfer)*, A. Kokhanovsky, Ed., pp. 71–114, Praxis Publishing, Chichester (2009).
40. J. W. Hovenier and D. W. Mackowski, "Symmetry relations for forward and backward scattering by randomly oriented particles," *J. Quant. Spectrosc. Radiat. Transfer* **60**, 483–492 (1998).
41. C. R. Hu et al., "Symmetry theorems on the forward and backward scattering Mueller matrices for light scattering from a nonspherical dielectric scatterer," *Appl. Opt.* **26**, 4159–4173 (1987).
42. A. Marciniak and B. Ciesielski, "EPR dosimetry in nails—a review," *Appl. Spectrosc. Rev.* **51**, 73–92 (2016).

**Sergey Savenkov** received his ScD degree from Taras Shevchenko National University of Kyiv, Ukraine, in 2013 and his PhD from Taras Shevchenko National University of Kyiv in 1996. Since 1986, he has been doing research at the Faculty of Radio Physics, Electronics and Computer Systems, Taras Shevchenko National University of Kyiv, Ukraine. His area of scientific interests includes laser polarimetry, polarimetry of anisotropic and depolarized media, and biomedical optics.

**Alexander Priezzhev** received his PhD from the Faculty of Physics, Lomonosov Moscow State University (MSU), Moscow, Russia, in 1971 and 1975, respectively. He is the head of the Laboratory of Laser Biomedical Photonics at MSU. He has led and participated in various national and international research projects on medical physics and biomedical optics, and published more than 250 papers in journals and conference proceedings. His areas of expertise include nanobiophotonics, biomedical optics, and physics of biological fluids.

**Yevgen Oberemok** received his PhD from the Faculty of Radio Physics, Electronics, and Computer Systems (before March 2014—Faculty of Radio Physics) of the Taras Shevchenko National University of Kyiv. His area of scientific interests includes experimental Stokes and Mueller polarimetry.

**Sergey Sholom** received his PhD from Kiev State University, Ukraine, in 1991. Since 2009, he has been doing research at the Physics Department of Oklahoma State University. His areas of scientific interest include emergency and accidental dosimetry of external exposure using different techniques (electron paramagnetic resonance, optically stimulated luminescence, thermoluminescence) in combination with different materials.

**Ivan Kolomiets** received his MSc degree from Taras Shevchenko National University of Kyiv, Ukraine, in 2012. Since 2010, he has been doing research at the Faculty of Radio Physics, Electronics, and Computer Systems, Taras Shevchenko National University of Kyiv, Ukraine. His areas of scientific interest include laser polarimetry, Mueller polarimetry of crystalline media, biomedical optics, and polarimetry.

**Kateryna Chunikhina** is currently receiving her BS degree at the Faculty of Radio Physics, Taras Shevchenko National University of Kyiv, Ukraine. Her scientific interests include Mueller polarimetry of crystalline media, biomedical optics, and polarimetry.